

Evolution of the subglacial drainage system beneath the Greenland Ice Sheet revealed by tracers

D. M. Chandler¹, J. L. Wadham^{1*}, G. P. Lis¹, T. Cowton², A. Sole³, I. Bartholomew², J. Telling¹, P. Nienow², E. B. Bagshaw¹, D. Mair⁴, S. Vinen⁵ and A. Hubbard⁶

Predictions of the Greenland Ice Sheet's response to climate change are limited in part by uncertainty in the coupling between meltwater lubrication of the ice-sheet bed and ice flow^{1–3}. This uncertainty arises largely from a lack of direct measurements of water flow characteristics at the bed of the ice sheet. Previous work has been restricted to indirect observations based on seasonal and spatial variations in surface ice velocities^{4–7} and on meltwater flux⁸. Here, we employ rhodamine and sulphur hexafluoride tracers, injected into the drainage system over three melt seasons, to observe subglacial drainage properties and evolution beneath the Greenland Ice Sheet, up to 57 km from the margin. Tracer results indicate evolution from a slow, inefficient drainage system to a fast, efficient channelized drainage system over the course of the melt season. Further inland, evolution to efficient drainage occurs later and more slowly. An efficient routing of water was established up to 41 km or more from the margin, where the ice is approximately 1 km thick. Overall, our findings support previous interpretations of drainage system characteristics, thereby validating the use of surface observations as a means of investigating basal processes.

The Greenland Ice Sheet is the largest reservoir of ice in the Northern Hemisphere, with the potential to contribute up to 7 m of sea-level rise³. An expanding volume of remote-sensing and global positioning system data has revealed wide variations in ice motion at sub-diurnal to inter-annual timescales, typically characterized by steady winter ice velocities and transient periods of fast flow during the summer melt season^{4–7,9–12}. Such speed-up events in land-terminating glaciers have been linked to periods of rapidly rising meltwater input^{4–7,9–12}.

Despite the short time span of observations in Greenland, there is good evidence to suggest that a key control on the relationship between meltwater input and faster ice flow is the subglacial drainage system efficiency^{5,7,13}. This is remarkably similar to the behaviour of much smaller valley glaciers extensively studied in the 1980s–1990s^{14–17}, in which faster basal motion caused by elevated subglacial water pressure occurs when the subglacial drainage system cannot accommodate rapid water inputs into moulins¹⁷. Elevated water pressure reduces the normal stress at the bed, lowering the friction opposing basal motion. Consequently, peak ice velocities often occur early in the melt season when the drainage system is poorly developed, and precede the period of peak melt. In Greenland, subglacial hydrological evolution is also driven by rapid drainages of surface lakes, which supply large but brief pulses of water to the ice sheet bed¹⁸. Unlike smaller valley

glaciers, where subglacial drainage development deduced from surface observations has been supported by extensive dye tracing evidence^{19–21}, our present understanding of Greenland's subglacial hydrology is based primarily on surface observations.

Assessing the impact of transient, hydrologically forced fast ice flow on ice sheet mass balance, and predicting how this impact might change under future climate warming scenarios, requires an improved understanding of relationships between subglacial hydrology and ice dynamics. Direct measurements of subglacial drainage system characteristics and development are needed to address this issue. Here we report results from artificial tracer experiments that provide the most direct evidence so far of efficient and inefficient drainage systems beneath the Greenland Ice Sheet.

Artificial tracers are commonly used in glaciology to investigate drainage systems in valley glaciers^{19–21}. Tracers are usually fluorescent dyes, which are highly soluble in water, can yield recovery rates >90% in suspended sediment-rich rivers²² and are conveniently measured automatically by fluorometry. However, fluorometer sensitivity (detection limit ~ 1 ppb; Supplementary Section S1) restricts the use of dye tracing at high dilution. Natural fluorescence of suspended sediments can also cause difficulties when separating the dye and suspended sediment signals in traces emerging over many hours. Owing to the large scale of the Greenland Ice Sheet melt zone, we expected tracer travel times and dilution to be much greater than those typical of Alpine glaciers. Therefore, we also employed sulphur hexafluoride gas (SF₆), which is commonly used in terrestrial and marine environments when dilution is high^{23–25}. To our knowledge, this is the first time SF₆ has been used to trace water flow in glacial systems. SF₆ has a much lower detection limit (here, 0.001 ppt in water) than rhodamine, is inert, does not interact with sediments, has a very low background concentration in the atmosphere (6.7 pptv in 2008²⁶) and is non-toxic.

Tracers were injected into moulins supplying the drainage system beneath a land-terminating outlet glacier in the Russell/Leverett catchment, West Greenland, at 67.0° N (Fig. 1). This region has been the subject of intensive recent research where diurnal- to seasonal-scale variations in ice surface velocity have been measured well into the accumulation zone^{5–7,9,10,12}. Results are reported from traces in three melt seasons (2009–2011) at sites 1.1–57 km from the glacier terminus (Fig. 1; Table 1). Tracer concentrations and water discharge were monitored in the single river emerging from the terminus (Supplementary Sections S1 and S3). Dye concentrations were monitored by fluorometer and SF₆ concentrations were determined in discrete river water samples

¹Bristol Glaciology Centre, School of Geographical Sciences, University of Bristol, Bristol BS8 1SS, UK, ²Department of Geography, School of Geosciences, University of Edinburgh, Edinburgh EH8 9XP, UK, ³Department of Geography, University of Sheffield, Sheffield S10 2TN, UK, ⁴Department of Geography and the Environment, School of Geoscience, University of Aberdeen, Aberdeen AB24 3UF, UK, ⁵School of Environmental Sciences, University of East Anglia, Norwich NR4 7TJ, UK, ⁶Institute of Geography and Earth Science, University of Aberystwyth, Aberystwyth SY23 3DB, UK. *e-mail: j.l.wadham@bris.ac.uk.

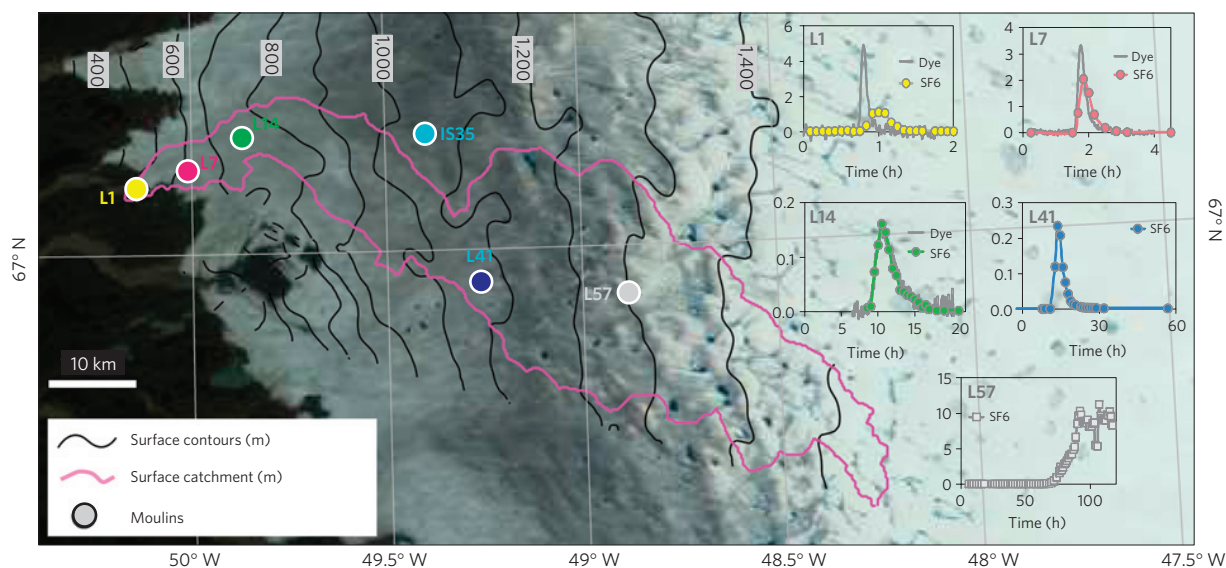


Figure 1 | Field site and example traces. **a**, MODIS (Moderate Resolution Imaging Spectroradiometer) image showing locations of moulins used for tracing, and the estimated boundary of the Leverett catchment (pink) calculated from a surface DEM (ref. 7). Insets: example dye and SF₆ traces at each site. Note the coherent dye and SF₆ returns from moulin L14 and a retarded SF₆ return from moulins L1 and L7. Tracer concentrations have been scaled to give unity area under the peaks, apart from the trace from L57 where the end of the SF₆ peak was not captured.

Table 1 | Locations of moulins used for tracer injections.

Moulin	Location	Distance from portal (km)	Surface elevation (m)	Ice thickness estimate (m)	Bed elevation (m)
L1	67° 04' N, 50° 09' W	1.1	377	45	332
L7	67° 05' N, 50° 01' W	6.8–7.1	579–611	380–460	119–231
L14	67° 07' N, 49° 52' W	13.9	790	670	130
IS39*	67° 07' N, 49° 24' W	39.0	1,061	1,100	–39
L41	66° 58' N, 49° 16' W	40.6	1,028	950–1,000 [†]	28–78
L57	66° 57' N, 48° 53' W	57.1	1,230	1,180	50

Surface elevations were measured by a handheld global positioning system (error approximately 5 m) and ice thickness was interpolated from NASA IceBridge ground penetrating radar data²⁹ (vertical resolution approximately 4.5 m on flight lines, and uncertainties clearly increasing away from flight lines) and from unpublished data collected by A.H. Bed elevation was estimated by subtracting ice thickness from surface elevation. *Site IS1 drained to Issunguata Sermia, the next major outlet to the north of the Leverett/Russell catchment. [†]Closest ice thickness data are ~500 m from L41.

analysed by gas chromatography with electron capture detector (Supplementary Section S1). Tracer velocities and other parameters were processed following methods in Supplementary Sections S1 and S2 and are reported in Supplementary Table S1.

Tracer returns from simultaneous SF₆ and dye traces showed similar maximum velocities, but mean velocities of SF₆ were often slower than those of dye owing to retardation of SF₆ in the drainage system (Supplementary Fig S2.7 and Table S1). Hence, only maximum velocities (v_{05} ; Supplementary Section S2) were used here to assess subglacial drainage system structure and development. Repeat traces of moulins at 7–41 km revealed increasing tracer velocities during the melt season (Fig. 2), with traces at 41 km initially emerging relatively slowly ($v_{05} = 0.25 \text{ m s}^{-1}$) but ultimately attaining a similar maximum velocity to those from 7 km ($v_{05} > 1 \text{ m s}^{-1}$; Fig. 2). This suggests evolution from a predominantly slow–inefficient, distributed drainage system to a predominantly fast–efficient channelized system at least 41 km from the margin, comparable with that observed in Alpine valley glaciers^{15–17}. These results are also consistent with time series of electrical conductivity and suspended sediment collected in the same proglacial river in 2009⁸. Further support for our interpretation is provided by the decreasing dispersion of dye traces from L7 and L14 as the season progressed (Supplementary Fig. S2.8), again similar to Alpine glaciers^{15–17}. The slow–inefficient system in the early melt season supports channel creep closure calculations that predict channels

close beneath most of the catchment over winter (Supplementary Section S4 and Fig. 2c). The very slow return ($v_{05} = 0.22 \text{ m s}^{-1}$) of a single trace from moulin L57 in late summer tentatively indicates that efficient drainage did not propagate this far inland, despite the drainage system having been able to evacuate similar moulin water fluxes at both L57 and L41 for at least five days before the trace at L57 (Supplementary Section S3.2). It is possible that the combination of relatively thick ice (~1,180 m) and periods of low water input to the moulin during the night (Supplementary Fig. S3.4) prevented development of an efficient system at L57.

Retardation of SF₆ relative to rhodamine in dual traces was strongest close to the ice margin and decreased inland (Fig. 2c), becoming negligible at L14. As both tracers were injected simultaneously, these contrasting characteristics must be a consequence of the tracer properties, most likely the high volatility of SF₆. Specifically, SF₆ will degas into headspace between the water below and the glacier above, similarly to in non-glacial environments²⁷. Subsequently, this SF₆ will partially redissolve into water that passes through later with a relatively lower SF₆ concentration, resulting in a retarded peak and long tail. Hence, SF₆ retardation can be used as a qualitative indication of the volume of air voids within the drainage system, which could be potentially linked to system pressurization. For example, SF₆ volatilization and consequent retardation will be greater in unpressurized englacial or subglacial channels with large headspaces than in water-

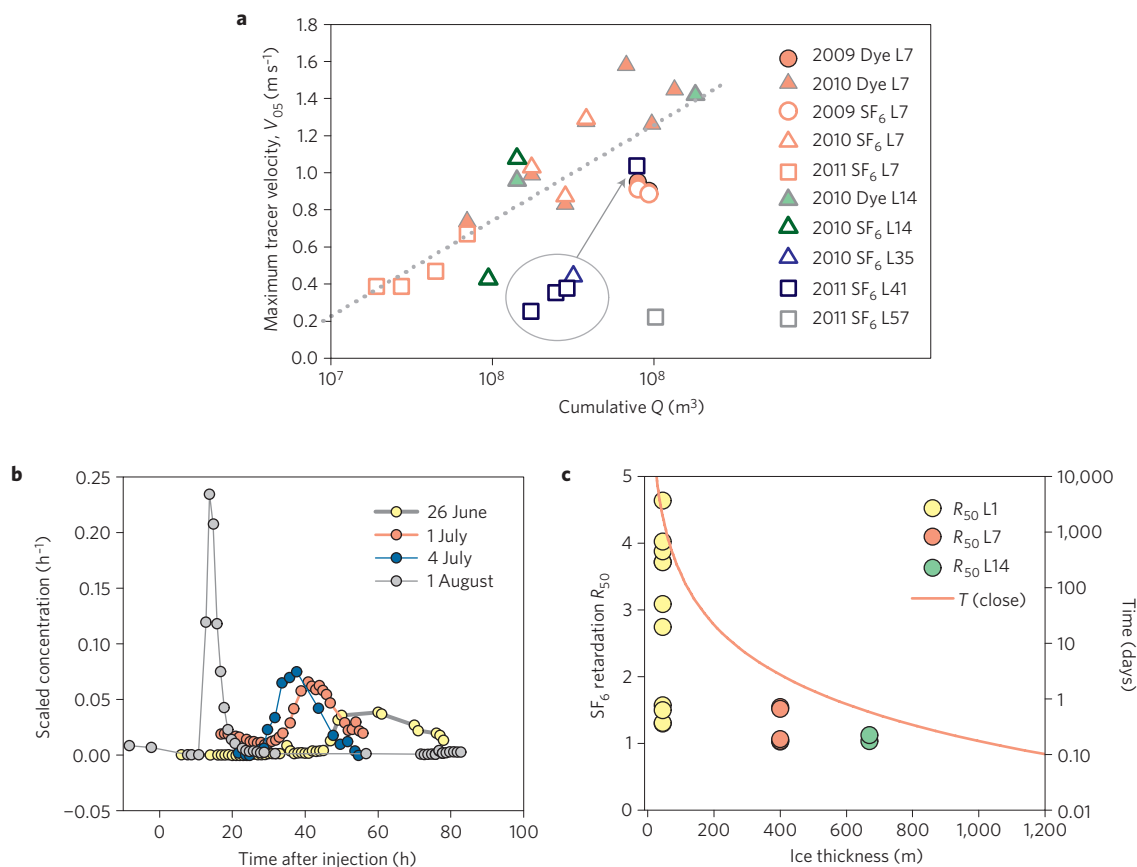


Figure 2 | Drainage system characteristics revealed by tracing. **a**, Evolution of tracer velocity with time. Cumulative discharge (ΣQ) is used to measure time because of variation in melt season onset and intensity between years (see Supplementary Fig. S3.1). The regression curve for maximum velocity (v_{05} ; Supplementary Section S2.3) from moulin L7 is $v_{05} = A \ln(\Sigma Q) + B$. **b**, Evolution of SF_6 traces at moulin L41 in 2011. **c**, Variation in SF_6 retardation R_{50} (Supplementary Section S2.4) with distance up-glacier from the terminus. The time taken for an empty channel to shrink to 1/10 of its original radius is also indicated (Supplementary Section S4).

filled, pressurized channels. The up-glacier decrease in retardation therefore suggests that the unpressurized zone is restricted to channels downstream of L7 (Fig. 2c). This is consistent with a single pressure record²⁸ from a borehole adjacent to a moulin located between L7 and L14, in which the subglacial water pressure stayed close to the ice overburden pressure well into the 2010 melt season. Although creep closure calculations provide further support for increasing channel pressurization upstream (see below), reverse bed slopes may also be a factor because channels must be pressurized upstream of any reaches where channel elevation increases in the downstream direction. Estimated bed elevations²⁹ indicate that reverse slopes are likely to exist (in particular between L1 and L7) but ice thickness measurements are patchy and off-transect valleys bisecting these reverse slopes cannot be ruled out.

Subglacial channel growth calculations derived from a simplified form of that presented in ref. 13 and applied here to the Leverett catchment (see Supplementary Section S4) yield timescales for channel development in reasonable agreement with our tracing observations. For example, with unlimited water supply (modelled by imposing subglacial water pressure equal to ice overburden pressure), estimated times taken for initially small (0.1 m^2 cross-section area) subglacial channels to double in size are 6, 23 and 28 days at L7, L41 and L57, respectively (Supplementary Fig. S4.2). At high sites, relatively slow development (due to thicker ice and shallower surface slope) and shorter melt seasons clearly hinder development of efficient drainage.

We note that the measured tracer velocities reflect drainage characteristics along the complete tracer trajectories, such that long

traces may include passages of both distributed and channelized flow. For example, the drainage system close to major meltwater inputs (moulins) at high sites may become channelized, even if there are long stretches of distributed flow between the moulin and channelized flow down-glacier (an analogy is a single river channel spreading out into a braided plain, before joining a more major river system). Stretches with slow flow, even if relatively short, will cause a disproportionately large increase in travel time³⁰.

Our direct observations of drainage system characteristics at Leverett Glacier strongly support previous interpretations of drainage system development derived from surface velocities in this region. For example, recent work at the same glacier⁶ showed that ice velocities at sites up to 1,229 m elevation responded most strongly to increasing surface melt during the early part of the melt season, after which velocities typically dropped to their winter values. This suggested an increasingly efficient drainage system in which melt inputs later in the season were more rapidly evacuated, such that greater melt volumes were needed to raise subglacial water pressure and increase sliding. Further, results indicated that this transient efficient fast flow (spring event) occurred later at higher elevations. Notably, our highest site (L57, where the drainage system remained slow–inefficient) is just beyond the upper limit of efficient drainage inferred from surface velocity patterns⁶. The use of surface velocities as a means of deducing basal hydrological conditions has been widely accepted for valley glaciers²⁰, and our tracing data now validate this approach for the Greenland Ice Sheet.

Our tracing results provide the most direct evidence so far for regions of efficient and inefficient meltwater drainage beneath

the Greenland Ice Sheet, and for the progressive up-glacier development of the drainage system during the melt season. At 67°N, meltwater transport is inefficient in the early melt season even at sites close to the margin (7 km), suggesting the previous year's drainage system becomes closed during the winter under most of the ablation zone. However, rapid development during the melt season led to efficient water routing up to at least 41 km from the margin, but not as far as 57 km. An important outcome of our study is the application of SF₆ as a tracer for measuring subglacial water velocity, which was successful at greater distances than are feasible with the fluorescent dyes normally employed in glaciology. Finally, whereas previous work in Greenland has yielded only qualitative information on drainage system characteristics, the quantitative data provided by our tracing results can now be used to validate models of ice-sheet hydrology.

Methods

Detailed descriptions of the methods used for tracer injection, tracer analysis, tracer data processing, monitoring of moulin discharge and modelling of channel growth are provided in Supplementary Information, Sections S1–S4, respectively. Ice thickness data were obtained from the IceBridge project, available at <http://nsidc.org/data/irmcr2.html>.

Received 22 June 2012; accepted 21 January 2013; published online 24 February 2013

References

- Gillet-Chaulet, F. *et al.* Greenland Ice Sheet contribution to sea-level rise from a new-generation ice-sheet model. *Cryosphere Discuss.* **6**, 2789–2826 (2012).
- Vaughan, D. G. & Athern, R. Why is it so hard to predict the future of ice sheets? *Science* **315**, 1503–1504 (2007).
- Solomon, S. *et al.* *Contribution of Working Group I to the Fourth Assessment Report of the Intergovernmental Panel on Climate Change* (Cambridge Univ. Press, 2007).
- Joughin, I. *et al.* Seasonal speedup along the western flank of the Greenland Ice Sheet. *Science* **320**, 781–783 (2008).
- Bartholomew, I. D. *et al.* Seasonal evolution of subglacial drainage and acceleration in a Greenland outlet glacier. *Nature Geosci.* **3**, 408–411 (2010).
- Bartholomew, I. D. *et al.* Seasonal variations in Greenland Ice Sheet motion: Inland extent and behaviour at higher elevations. *Earth Planet. Sci. Lett.* **307**, 271–278 (2011).
- Palmer, S., Shepherd, A., Nienow, P. & Joughin, I. Seasonal speedup of the Greenland Ice Sheet linked to routing of surface water. *Earth Planet. Sci. Lett.* **302**, 423–428 (2011).
- Bartholomew, I. D. *et al.* Supraglacial forcing of subglacial drainage in the ablation zone of the Greenland ice sheet. *Geophys. Res. Lett.* **38**, L08502 (2011).
- Van de Wal, R. S. W. *et al.* Large and rapid melt-induced velocity changes in the ablation zone of the Greenland Ice Sheet. *Science* **321**, 111–113 (2008).
- Shepherd, A. *et al.* Greenland Ice Sheet motion coupled with daily melting in late summer. *Geophys. Res. Lett.* **36**, L01501 (2009).
- Hoffman, M. J., Catania, G. A., Neumann, T. A., Andrews, L. C. & Rumrill, J. A. Links between acceleration, melting, and supraglacial lake drainage of the western Greenland Ice Sheet. *J. Geophys. Res.* **116**, F04035 (2011).
- Sundal, A. V. *et al.* Melt-induced speed-up of Greenland ice sheet offset by efficient subglacial drainage. *Nature* **469**, 521–524 (2011).
- Schoof, C. Ice-sheet acceleration driven by melt supply variability. *Nature* **468**, 803–806 (2010).
- Iken, A. & Bindschadler, R. A. Combined measurements of subglacial water pressure and surface velocity of Findelengletscher, Switzerland: Conclusions about drainage system and sliding mechanism. *J. Glaciol.* **32**, 101–119 (1986).
- Nienow, P. W., Sharp, M. & Willis, I. C. Seasonal changes in the morphology of the subglacial drainage system, Haut Glacier d'Arolla, Switzerland. *Earth Surf. Process.* **23**, 825–843 (1998).
- Jansson, P. Dynamics and hydrology of a small polythermal valley glacier. *Geogr. Ann.* **78A**, 171–180 (1996).
- Mair, D. *et al.* Hydrological controls on patterns of surface, internal and basal motion during three spring events: Haut Glacier d'Arolla, Switzerland. *J. Glaciol.* **49**, 555–567 (2003).
- Das, S. B. *et al.* Fracture propagation to the base of the Greenland Ice Sheet during supraglacial lake drainage. *Science* **320**, 778–781 (2008).
- Seaberg, S. Z., Seaberg, J. Z., Hooke, R. LeB. & Wieberg, D. Character of the englacial and subglacial drainage system in the lower part of the ablation area of Storglaciären, Sweden, as revealed by dye-trace studies. *J. Glaciol.* **34**, 217–227 (1988).
- Hubbard, B. & Nienow, P. Alpine subglacial hydrology. *Quat. Sci. Rev.* **16**, 939–955 (1997).
- Bingham, R. G., Nienow, P. W., Sharp, M. J. & Boon, S. Subglacial drainage processes at a High Arctic polythermal valley glacier. *J. Glaciol.* **51**, 15–24 (2005).
- Smart, P. L. & Laidlaw, I. M. S. An evaluation of some fluorescent dyes for water tracing. *Wat. Resour. Res.* **31**, 15–33 (1977).
- Watson, A. J., Liddicoat, M. I. & Ledwell, J. R. Perfluorodecalin and sulphur hexafluoride as purposeful marine tracers: Some deployment and analysis techniques. *Deep-Sea Res.* **34**, 19–31 (1987).
- Clark, J. F., Schlosser, P., Stute, M. & Simpson, H. J. SF₆ – ³He tracer release experiment: A new method of determining longitudinal dispersion coefficients in large rivers. *Environ. Sci. Technol.* **30**, 1527–1532 (1996).
- Dillon, K. S., Corbett, D. R., Chanton, J. P., Burnett, W. C. & Kump, L. Bimodal transport of a waste water plume injected into saline ground water of the Florida Keys. *Ground Wat.* **38**, 624–634 (2000).
- Rigby, M. *et al.* History of atmospheric SF₆ from 1973–2008. *Atmos. Chem. Phys.* **0**, 10305–10320 (2010).
- Upstill-Goddard, R. C. & Wilkins, C. S. The potential of SF₆ as a geothermal tracer. *Wat. Resour. Res.* **29**, 1065–1068 (1995).
- Smeets, C. J. P. *et al.* A wireless subglacial probe for deep ice applications. *J. Glaciol.* **58**, 841–848 (2012).
- Allen, C. *IceBridge MCoRDS L2 Ice Thickness* [2010, 2011]. Boulder, Colorado, USA: NASA DAAC at the National Snow and Ice Data Center. Digital media. <http://nsidc.org/data/irmcr2.html> (2010, updated current year).
- Nienow, P., Sharp, M. & Willis, I. Velocity–discharge relationships derived from dye tracer experiments in glacial meltwaters: Implications for subglacial flow conditions. *Hydrol. Process.* **10**, 1411–1426 (1996).

Acknowledgements

This work was supported by the Leverhulme Trust (Phillip Leverhulme Prize to J.L.W.), UK NERC grant NE/H023879/1 to J.L.W., NERC NE/F021380/1 grant to P.N., NERC grant NE/G005796/1 to A.H., financial support from the Greenland Analogue Project and SKB/Positiva to A.H., and Moss Scholarships to T.C. and I.B. We thank the Atmospheric Chemistry Research Group at the University of Bristol who aided with SF₆ analysis in the early stages of the project. We acknowledge the use of ice thickness data collected by the NASA IceBridge project. We thank Hozelock for supplying hoses, and are grateful to the many field assistants who have contributed to the collection of field data.

Author contributions

D.M.C. designed the tracer experiments in the field and conducted tracer data analysis, developed the model of drainage evolution and co-wrote the manuscript. J.L.W. led the project, designed the tracer experiments in the field and conducted tracer data analysis, and co-wrote the manuscript with D.M.C. G.P.L., S.V. and J.T. were responsible for SF₆ analysis by gas chromatography and method development. P.N., D.M.C., A.S., T.C. and I.B. contributed discharge and dye tracing data, and input to writing of the manuscript. E.B.B. contributed to field logistics and input to writing of the manuscript. A.H. was responsible for in-field support of the campaign, provided ice thickness data and input to writing of manuscript.

Additional information

Supplementary information is available in the [online version of the paper](#). Reprints and permissions information is available online at www.nature.com/reprints. Correspondence and requests for materials should be addressed to J.L.W.

Competing financial interests

The authors declare no competing financial interests.